ELSEVIER

Materials Science and Engineering A241 (1998) 259–263

MATERIALS SCIENCE & ENGINEERING A

Gradient microstructure in laser clad TiC-reinforced Ni-alloy composite coating

Y.T. Pei *, T.C. Zuo

National Center of Laser Technology, Beijing Polytechnic University, Beijing 100022, People's Republic of China

Received 5 November 1996; received in revised form 23 June 1997

Abstract

A gradient TiC–(Ni alloy) composite coating was produced by one step laser cladding with pre-placed mixture powder on a 1045 steel substrate. The clad layers consisted of TiC particles, γ-Ni primary dendrites and interdendritic eutectics. From the bottom to the top of the clad layer produced at 2000 W laser power and 6 mm s^{-1} scanning speed, TiC particles exhibited a continuous increase both in size (from 0.8 to 4.8 μm) and in volume fraction (from 1.72 to 32.8%). Their morphology changes from small globe to coarse flower-like cluster. Laser processing parameters have a considerable influence on the gradient distribution of TiC particles in the clad layers. © 1998 Elsevier Science S.A.

Keywords: Gradient microstructure; TiC particles; Ni alloy; Composite coating; Laser cladding

1. Introduction

A common method to improve the performance of a component is coating a bulk material for use in severe environments. However, the coating material and the substrate typically have different physical and mechanical properties and as a result, interface is one of the possible failure modes. The concept of functionally gradient materials (FGMs), in which the controlled progressive changes are presented both in structure and properties, is pursued in materials development in order to avoid the problem due to interface [1,2].

Jasim et al. [3] reported a functionally gradient coating (FGC) built up by three vertically overlapping laser-processed tracks, in which the proportion of SiC reinforcement increased in steps from 10 to 50 vol.%. Their work showed the possibility of laser processing to deposit a thick multilayer of essentially discrete composition other than a gradual composition change. Abboud et al. [4,5] presented details of a Ti–Al functionally gradient clad, produced by the same technique as the above, with less 'severe' discontinuities of composition and structure. Unfortunately, there were sharp demarcations between the layers, which created sudden changes in material properties across the whole coating. Similar studies were also done by others [6,7].

In this work, a composite coating with continuous gradient microstructure was produced by one-step laser cladding from the mixed powders of 30 vol.% TiC plus 70 vol.% Ni-alloy. Utilizing the movement of partially-dissolved TiC particles (TiC_p) in the laser molten pool and their regrowth upon resolidification, a gradient distribution of TiC_p within the composite coating was achieved. The exploratory investigation reported here deals only with the microstructural features of the coating and tests an alternative approach, which is different from the above to obtain a FGC. The optimization of laser-processing parameters and of clad material systems still requires further investigation.

2. Experimental details

The 50 mm × 40 mm × 10 mm strips of commercial steel 1045 were used as substrate. These strips were ground with 200-grid SiC abrasive paper and cleaned with acetone before laser cladding. TiC particles were chosen as the ceramic reinforcement for their potential for improving wear resistance. In addition, their partially dissolution and regrowth behavior during laser processing [8] is beneficial to form a FGC. Ni–Cr–B–

* Corresponding author.

PII S0921-5093(97)00501-7

Si alloy was selected as the matrix of the composite coating because of its good resistance against corrosion and erosion as well as its fine compatibility with TiC_p. The average particle size of raw powders was 2 and 30 μm for TiC_p and Ni-alloy respectively. The chemical composition of Ni-alloy was (wt.%): 15.0Cr, 4.0B, 5.8Si, 0.73C, 12.3Fe and Ni in balance. The thickness of the pre-placed mixture powders on the substrate was about 1 mm.

A 2.5 kW continuous wave CO_2 laser was employed to produce a series of single clad tracks without overlap under the processing conditions of 1800–2200 W laser power, 4–8 mm s^{-1} scanning speeds of laser beam and 3 mm beam diameter. Argon was blown to shroud the molten pool from the outside atmosphere.

The transverse sections of the clad tracks were cut for microstructural studies. Electrolytic etching with a 1 mol% NaOH solution was first used to attack the clad layer of the composite coating, then 4% nital was chosen to reveal the heat affected zone of the substrate. Microstructural observations were carried out using a Hitachi S570-type scanning electron microscope (SEM) and a Philips CM-12 type transmission electron microscope (TEM), both being equipped for energy dispersive X-ray analysis (EDXA).

3. Results and discussion

Fig. 1 shows the cross section of a single track of laser clad 30 vol.% TiC_p-(Ni alloy) composite coating on the steel substrate. The transverse view of the track is arched and its maximum thickness is about 600 μm. The general appearance of the clad layer is very good, without any problem of adherence, porosity or cracks on the section.

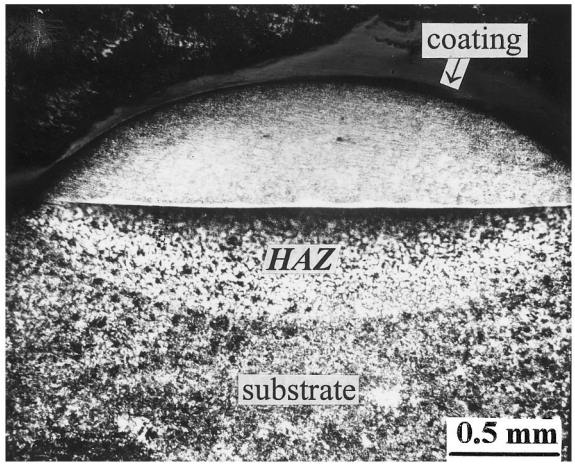

Fig. 1. Transverse section of laser clad 30 vol.% TiC–(Ni alloy) composite coating.

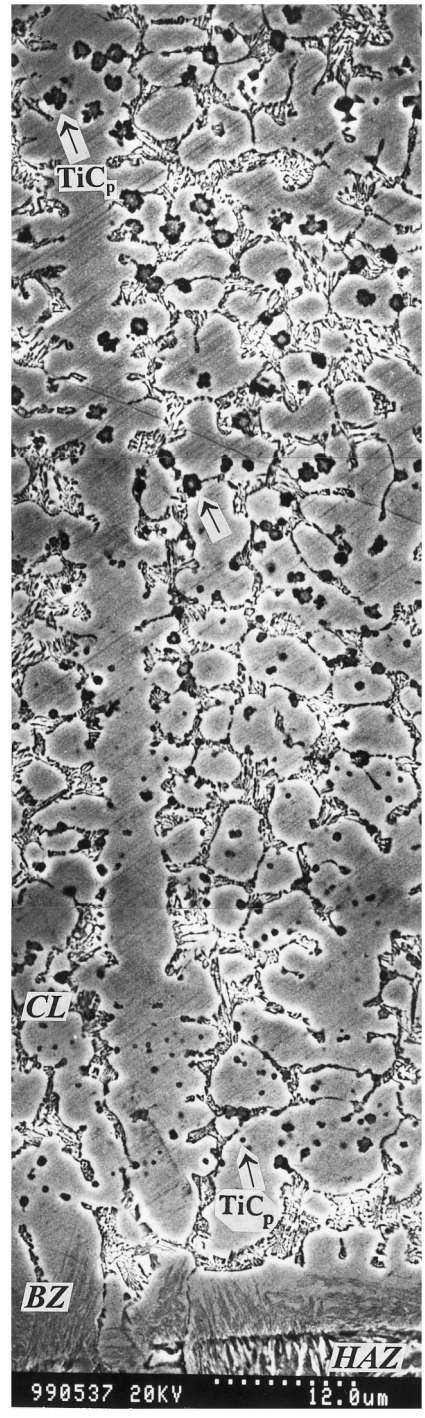

Fig. 2. Gradient microstructure of 30 vol.% TiC–(Ni alloy) composite coating clad at 2000 W laser power and 6 mm s^{-1} scanning speed. (All the arrows indicate TiC_p.)

The microstructure of the composite coating is revealed in Fig. 2. The bonding zone (labeled BZ) about which is 10 μm thick presents excellent fusion bond between the clad layer (labeled CL) and the heat affected zone of substrate (labeled HAZ). The clad layer exhibits γ-Ni primary dendrites, interdendritic eutectics and a large amount of TiC particles. In general,

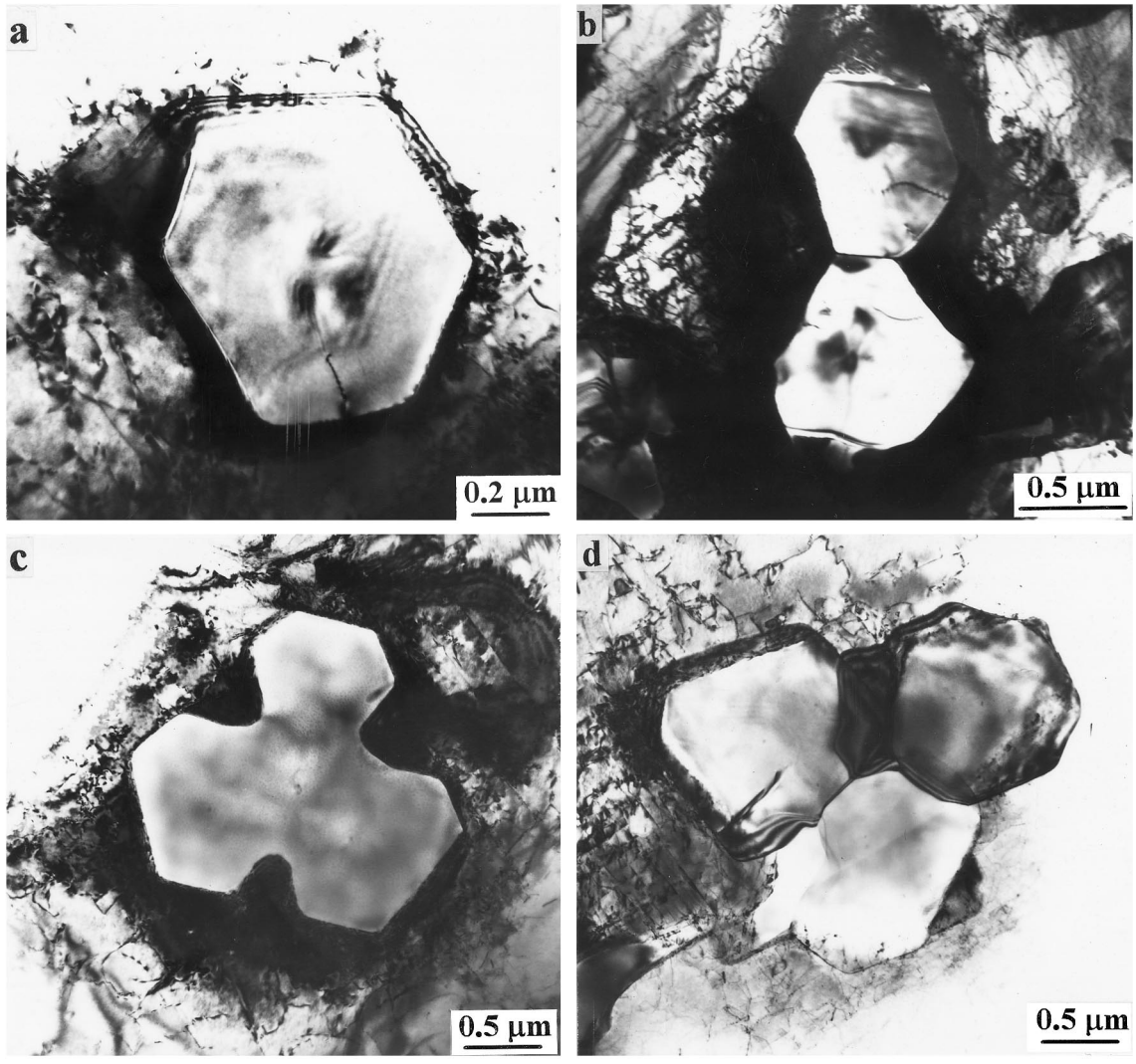

Fig. 3. TEM micrographs showing the growing features of TiC_p in different regions of the layer clad at 2000 W laser power and 6 mm s^{-1} scanning speed: (a) at bottom; (b) at lower part; (c) at intermediate part; (d) at upper part.

these TiC particles are distributed homogeneously throughout the whole layer. However, the size of the particles changes continuously with location moving upwards from the bottom of the layer. SEM micrographs presented in Fig. 2 indicate an increase of approximately three times in the average size of TiC_p over 120 μm distance, moving upwards from the CL/BZ interface. Moreover, the morphology of TiC_p varies from global to flower-like shape. These characteristics of TiC_p strongly signify that the particles must be clustered in laser pool, since a common growth mechanism involving solute diffusion through the melt can not play such an important role in the enlargement of TiC_p during the rapid solidification of laser pool.

TEM micrographs in Fig. 3 show clearly the growing features of TiC_p both in size and morphology. At the bottom of the clad layer, individual TiC particles are found with hexahedral geometry (Fig. 3(a)), which should be formed by a lateral spreading mechanism and finally surrounded with the low index faces of TiC cubic crystals [9]. Their sizes are about 0.8 μm and much smaller than that of the raw powders. This is evidence of the partial dissolution of TiC primary particles in the laser molten pool. Fig. 3(b) presents two particles stuck without coalescence in the lower region of the clad layer. It is considered that at the early stage of solidification of the pool, there is a chance for TiC_p to collide with each other and only sticking between them can occur before they are engulfed by the growing liquid–solid front. The typical flower-like clusters of TiC_p are observed in the middle and upper region of the clad layer, as shown in Fig. 3(c) and (d), which support the SEM results. Partial sintering of TiC particles by their growth to the center of the clusters takes place due to the precipitation of TiC content from the supersaturated melt.

The detailed information about the gradient distribution of TiC_p in the whole layer are given in Fig. 4. According to the result of polynomial regression, the sizes of TiC_p cluster increase according to the formula:

$$S_p = 0.708 + 1.26 \times 10^{-2} d - 9.69 \times 10^{-6} d^2,$$

where S_p represents the cluster size, and d indicates the distance from the location of clusters to the CL/BZ interface. Obviously, the growth of clusters in the later stage of solidification becomes slower because the newly collided particles will fill the vacant positions among the members of a multi-membered cluster formed in the early stage. On the other hand, the interparticle spacing has only a linear increase with the distance. This means that the volume fraction of TiC_p in a local region of the layer increases as a cubic function of d, changing from 1.72% at the bottom of the layer to 32.8% at the top of the layer. However, the average volume fraction of TiC_p in the whole layer is about 14.5%, which is only half of the original content in the mixture powder. Besides these regrown TiC_p in the melt, it was found in previous work that there were a large amount of TiC precipitates from γ-Ni solid solution, but their sizes were not larger than 0.1 μm. [10]

Laser processing parameters exert a considerable influence on the gradient distribution of TiC_p. Fig. 5 shows the microstructure of the composite coating produced at 2200 W laser power and 8 mm s^{-1} scanning speed. The increase in TiC_p size with location within the CL is not so significant, compared with that in Fig. 2. Only twice the average size of TiC_p can be observed on the micrographs in Fig. 5, which covers nearly the same wide region of the CL moving upward from the CL/BZ interface as Fig. 2. This is mainly attributed to the shorter period of time it takes for TiC particles to regrow and to be clustered within the melt at higher scanning speed of laser beam. It is expected that the precipitation of Ti and C elements, coming from the partial dissolution of TiC primary particles in the laser molten pool, will be more incomplete from the matrix. EDXA results given in Table 1 prove that all γ-Ni dendrites in the whole layer clad at 8 mm s^{-1} scanning speed are more severely saturated with Ti than those formed at 6 mm s^{-1} scanning speed.

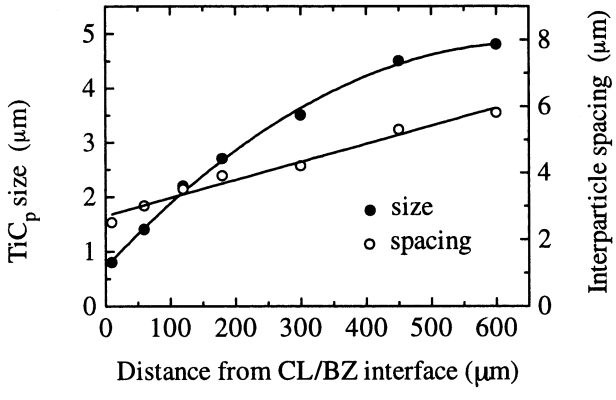

Fig. 4. Continuous increase of TiC_p sizes and interparticle spacing with the distance from their location to the CL/BZ interface (cladding parameters: 2000 W laser power and 6 mm s^{-1} scanning speed).

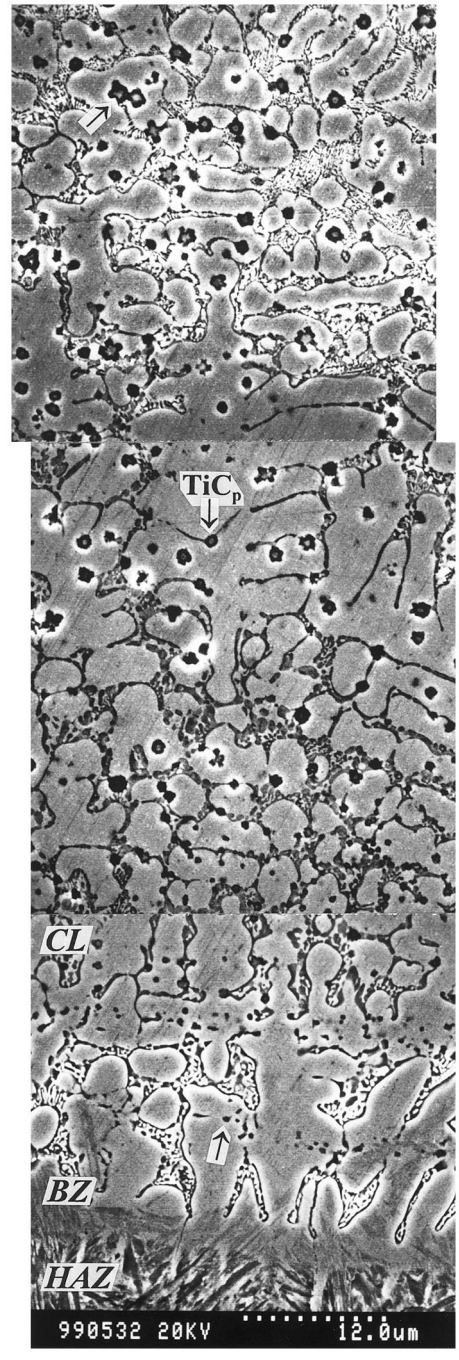

Fig. 5. Gradient microstructure of 30 vol.% TiC–(Ni alloy) composite coating clad at 2200 W laser power and 8 mm s^{-1} scanning speed. (All the arrows indicate TiC_p.)

Table 1
Composition of γ-Ni dendrites in different regions of the layers determined by EDXA

Scanning speed of laser beam (mm s^{-1})	Region of layer	Composition[a], wt.%				
		Ni	Cr	Fe	Si	Ti
6	Upper	62.9	12.2	17.6	4.5	2.8
	Intermediate	57.8	12.5	21.4	4.8	3.5
	Bottom	50.6	9.6	31.2	3.7	4.9
8	Upper	62.5	13.6	15.4	4.8	3.7
	Intermediate	61.7	12.9	17.2	4.0	4.2
	Bottom	54.6	11.4	24.7	4.1	5.2

[a] With C, B excluded.

4. Conclusions

(1) By one step laser cladding, a gradient TiC_p/Ni-alloy composite coating can be obtained. The clad layer consists of TiC particles, γ-Ni primary dendrites and interdendritic eutectics.

(2) From the bottom to the top of the clad layer, TiC particles exhibit a continuous increase both in size and volume fraction, and their morphology changes correspondingly from small globe to coarse flower-like cluster.

(3) Less significant growth in TiC_p size with location is observed in the layer clad at higher scanning speed of laser beam.

Acknowledgements

This work was supported by the Natural Science Foundation of China (No.59601012) and partially supported by the Young Scientist Foundation of Beijing.

References

[1] M. Nino, S. Maeda, ISIJ Int. 30 (1990) 699.
[2] T. Hirai, M. Sasaki, JSME Int. 34 (1991) 123.
[3] K.M. Jasim, R.D. Rawlings, D.R.F. West, J. Mater. Sci. 28 (1993) 2820.
[4] J.H. Abboud, R.D. Rawlings, D.R.F. West, Mater. Sci. Technol. 10 (1994) 414.
[5] J.H. Abboud, D.R.F. West, R.D. Rawlings, Mater. Sci. Technol. 10 (1994) 848.
[6] A. Schueßler, in: B.L. Mordike (Ed.), Laser Treatment of Materials (ECLAT '92), DGM, Oberursel, Germany, 1992, pp. 287–292.
[7] P. Wu, C.Z. Zhou, X.N. Tang, Surf. Coat. Technol. 73 (1995) 111.
[8] T.C. Lei, J.H. Ouyang, Y.T. Pei, Y. Zhou, Mater. Sci. Technol. 11 (1995) 520.
[9] M.C. Flemings, Solidification Processing, McGraw-Hill, New York, 1974, pp. 319–324.
[10] Y.T. Pei, Q.C. Men, J.H. Ouyang, T.C. Lei, Chinese J. Lasers A22 (1995) 935.